

SELF-CALIBRATING TRIANGULATION OF AIRBORNE LINEAR ARRAY CCD CAMERAS

S. Kocaman, L. Zhang, A. Gruen

Institute of Geodesy and Photogrammetry, ETH Hoenggerberg, CH-8093 Zurich, Switzerland
(skocaman, zhangl, agruen)@geod.baug.ethz.ch

KEY WORDS: Airborne Linear Array Cameras, Triangulation, Self-calibration.

ABSTRACT:

Since their first introduction, linear array CCD cameras play an important role in the airborne optical digital sensors market, together with matrix array CCD sensors. Most of the aerial linear array cameras work with the three-line-scanner (TLS) principle. The methods and algorithms to process airborne linear array imagery opened a wide research area to the scientists due to its fairly new geometry and the use of data from auxiliary sensors. To make efficient use of airborne linear array sensors, new processing methods needed to be developed and the existing ones re-designed. Algorithms and software for a complete photogrammetric processing chain for TLS imagery have been developed at our Institute, ETH Zurich, since the year 2000. For the triangulation of TLS imagery, a modified bundle adjustment algorithm with the possibility of use of three different trajectory models was developed (Gruen and Zhang, 2002) and in the meantime tested with data of several sensors.

Self-calibration is an efficient and powerful technique used for the calibration of photogrammetric imaging systems for over 30 years. Systematic error models of conventional single frame aerial cameras for aerial photogrammetry and digital cameras for close-range photogrammetry have already been defined and sufficiently discussed by several authors. As a new-generation imaging sensor, the systematic error sources of the linear array sensors should be identified and discussed accordingly. In this research, the potential systematic error sources of the airborne linear array sensor imagery are examined and the self-calibration capabilities of the TLS sensors are investigated by introducing 16 additional parameters (AP) to the basic TLS sensor model. After preliminary investigations under various test networks, undeterminable APs are removed from the initial set. An iterative algorithm, which eliminates undeterminable parameters from the full-set during the bundle adjustment for optimal estimation of point coordinates, and under arbitrary network conditions, is developed. In this algorithm, the covariance matrix of unknowns is analyzed in terms of determinability, parameter correlation, and parameter significance using appropriate statistical methods. The software and the parameters are tested using testfield data acquired by different models of the STARIMAGER sensors from former Starlabo Corporation, Tokyo, and the ADS40 sensor from Leica Geosystems, Heerbrugg. In this paper, the mathematical model of the linear array self-calibration and the first test results are presented. It is shown that self-calibration can improve the results of triangulation significantly.

1. INTRODUCTION

The introduction of digital line sensors into the field of aerial photogrammetry has provided a challenging research area for photogrammetrists due to its fairly new sensor geometry and wide-range of spectral data availability. Cameras based on linear CCD sensors like the Wide Angle Airborne Camera WAAC (Boerner et al., 1997), the High Resolution Stereo Camera HRSC (Wewel et al., 1999), the Digital Photogrammetric Assembly DPA (Haala et al., 1998) were the first digital systems being used for airborne applications. The first commercial line scanner Airborne Digital Sensor ADS40 was developed by LH Systems jointly with DLR (Reulke et al., 2000, Sandau et al., 2000). In the year 2000, Starlabo Corporation, Tokyo designed a new airborne digital imaging system, the Three-Line-Scanner (TLS) system, jointly with the Institute of Industrial Science, University of Tokyo and completed in the meantime several test flights. The TLS system was originally designed to record line features (roads, rivers, railways, power-lines, etc) only, but later tests also revealed the suitability for general mapping and GIS-related applications (Murai and Matsumoto, 2000). The system was lately called as STARIMAGER and four engineering models, namely SI-100, SI-250, SI-290, and SI-290N, with varying numbers of CCD lines and numbers of pixels in each, have been presented by Starlabo Corporation.

Recently, two new aerial linear array CCD cameras, 3-DAS-1 from Wehrli Associates and JAS-150 from Jena-Optronik, have been introduced into the market. However, no test flights from these sensors are available up to now.

Although substantial literature on the sensor geometry and systematic error sources of conventional aerial and terrestrial frame cameras exists, further investigations on these topics for the linear array CCD sensors are still necessary. Each scan line of the linear array CCD image is collected in a pushbroom fashion at a different instant of time. Therefore, and in principle, there is a set of exterior orientation parameters associated with each scan line. Our TLS sensor model is based on modified collinearity equations and uses different forms of trajectory models. Three different types of trajectory models have already been addressed by Gruen and Zhang (2002): (a) *Direct georeferencing* with stochastic exterior orientations (*DGR*), (b) *Piecewise Polynomials* with kinematic model up to second order and stochastic first and second order constraints (*PPM*) and (c) *Lagrange Polynomials* with variable orientation fixes (*LIM*). These models are used for the improvement of the exterior orientation parameters, which are measured by a high accuracy GPS and INS system by a modified photogrammetric bundle adjustment procedure, called TLS-LAB (Gruen and Zhang, 2002). A number of ground control points are needed for this approach in order to achieve high accuracies.

Self-calibration is an efficient and powerful technique used for calibration of photogrammetric imaging systems. If used in the context of general bundle solution, it provides for object space coordinates or object features, camera exterior and interior orientation parameters, and models systematic errors as well (Gruen and Beyer, 2001). It has now been more than 30 years since the concept of camera system self-calibration was introduced into the photogrammetric community. Systematic error models of conventional aerial cameras for aerial photogrammetry and digital cameras for close-range photogrammetry have already been defined by several authors (Ebner, 1976; Brown, 1976; Gruen, 1978; Beyer, 1992; Fraser, 1997). As a new-generation imaging sensor, a set of systematic error parameters of the TLS sensors are identified and discussed in this paper. The proposed self-calibration model is integrated into the trajectory models and developed under the TLS-LAB software. The model is tested in practical applications using two different datasets acquired by ADS40 and SI-100 sensors, and the results are discussed.

2. THE MATHEMATICAL MODEL

2.1 TLS Trajectory Models

The TLS sensor model has been described by several authors (Chen et al, 2001, 2003; Gruen and Zhang, 2002, 2003). Three trajectory models have been implemented by Gruen and Zhang (2002) for this purpose. However, only two of them, DGR and LIM, are extended for the use of self-calibration.

The observation equations used for the least squares adjustment with the DGR model are:

$$\begin{aligned} v_c &= Ax_{off} + B_s x_s + B_d x_d + Cx_g - l_c ; P_c \\ v_s &= \quad \quad \quad x_s \quad \quad \quad -l_s ; P_s \\ v_d &= \quad \quad \quad \quad \quad x_d \quad \quad \quad -l_d ; P_d \\ v_g &= \quad \quad \quad \quad \quad \quad \quad x_g \quad -l_g ; P_g \end{aligned} \quad (1)$$

The first equation of this system is the linearized observation equation of the basic triangulation equations combined with the collinearity equation, x_{off} is the unknown positional offset vector of GPS measurements; x_s and x_d are the unknown INS shift and drift terms respectively; x_g is the ground coordinates vector; A , B_s , B_d , and C are the corresponding design matrices; v , l and P are the respective residual and discrepancy vectors and weight matrices.

With the LIM, the exterior orientation parameters are determined in the so-called orientation fixes, which are introduced at certain time intervals. Between the orientation fixes, the exterior orientation parameters of an arbitrary scan line are interpolated using Lagrange polynomials. This method has been developed by Ebner et al. (1992) for orientation of MOMS images, and modified by Gruen and Zhang (2002) according to the TLS sensor model with the provision of auxiliary position/attitude data generated by the GPS/INS system. The following observation equations are used for the combined triangulation procedure:

$$\begin{aligned} v_c &= Ax_a + Bx_{INS} \quad \quad \quad + Cx_g - l_c ; P_c \\ v_t &= \quad \quad \quad x_{INS} + B_s x_s + B_d x_d - l_t ; P_t \\ v_s &= \quad \quad \quad \quad \quad x_s \quad \quad \quad -l_s ; P_s \\ v_d &= \quad \quad \quad \quad \quad \quad \quad x_d \quad \quad \quad -l_d ; P_d \\ v_g &= \quad \quad \quad \quad \quad \quad \quad \quad \quad x_g \quad -l_g ; P_g \end{aligned} \quad (2)$$

where the first equation of this system is the linearized observation equation of basic triangulation equations, the second

one is a constraint which models the INS error terms in the whole trajectory as shift and drift terms. P_t controls the weight of this constraint. x_a is the unknown attitude parameter vector (Ω , Φ , K) of the aircraft for the orientation fixes; x_{INS} is the unknown INS error vector ($\Delta\omega$, $\Delta\varphi$, $\Delta\kappa$) for the orientation fixes; x_s and x_d are the unknown INS shift and drift terms respectively; x_g is the ground coordinates vector; A , B_s , B_d , and C are the corresponding design matrices; v , l and P are the respective residual and discrepancy vectors and weight matrices.

2.2 Self-calibration Parameters

Chen et al. (2003) described the CCD line structure and calibration of the TLS camera. Starting from this point, a total of 16 additional parameters (APs) are identified, implemented, and tested in the TLS-LAB software. The CCD line structure in the image coordinate system is given in Figure 1.

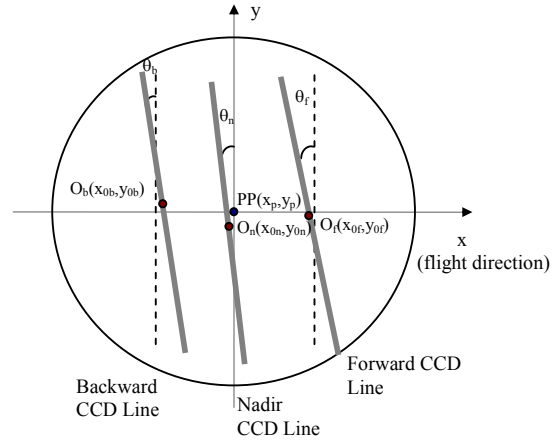


Figure 1. CCD line structure of the TLS camera. (x, y) denote the image coordinate system. O_b , O_n , and O_f denote the CCD line centers, and θ_b , θ_n and θ_f are the inclination angles with the y axis for the backward, nadir and forward CCDs, respectively. PP represents the principal point of the camera lens.

The initial AP set consists of:

(Δc) : Systematic error in the focal length of the camera lens.

$(\Delta x_{pb}, \Delta x_{pf})$: Displacements of the line centers of the backward and forward CCDs from the principle point (PP) of the camera lens, defined in the flight direction.

$(\Delta y_{pb}, \Delta y_{pf})$: Displacements of the line centers of the backward and forward CCDs from the principle point (PP) of the camera lens, defined across the flight direction.

Lens Distortion Parameters: Radial symmetric lens distortion (k_1, k_2, k_3) and decentering distortion (p_1, p_2) models of Brown (1971).

(s_{yb}, s_{yn}, s_{yf}) : Affinity is defined in x direction by Beyer (1992) for close-range frame CCD cameras. In this study, affinity parameters for each CCD line are used in the (y) direction.

$(\Delta\theta_b, \Delta\theta_n, \Delta\theta_f)$: The $\Delta\theta$ parameters represent the systematic error of the inclination angle between each CCD line and the (y) axis of the camera coordinate system (Figure 1). The effect of $\Delta\theta$ on the y -coordinates is discarded due to the small error magnitude.

The functional model for self-calibration for the TLS backward and forward images are described as follow:

$$\Delta x_{i<b,f>} = \Delta x_p - \frac{(x_i - x_p)}{c} \Delta c + (x_i - x_p) r_1^2 k_1 + (x_i - x_p) r_1^4 k_2 + (x_i - x_p) r_1^6 k_3 + (r_1^2 + 2(x_i - x_p)^2) p_1 + 2(x_i - x_p)(y_i - y_p) p_2 + \frac{(y_i - y_p)}{\rho} \Delta \theta_{<b,f>} \quad (3)$$

$$\Delta y_{i<b,f>} = \Delta y_p - \frac{(y_i - y_p)}{c} \Delta c + (y_i - y_p) r_1^2 k_1 + (y_i - y_p) r_1^4 k_2 + (y_i - y_p) r_1^6 k_3 + (r_1^2 + 2(y_i - y_p)^2) p_2 + 2(x_i - x_p)(y_i - y_p) p_1 - (y_i - y_p) s_{y<b,f>} \quad (4)$$

where;

x_i, y_i : image coordinates of each point,
 x_p, y_p : image coordinates of the principal point of the lens,
 $\rho = 180/\pi$
 $r_1^2 = (x_i - x_p)^2 + (y_i - y_p)^2$

The functional model for the TLS nadir image is:

$$\Delta x_n = - \frac{(x_i - x_p)}{c} \Delta c + (x_i - x_p) r_1^2 k_1 + (x_i - x_p) r_1^4 k_2 + (x_i - x_p) r_1^6 k_3 + (r_1^2 + 2(x_i - x_p)^2) p_1 + 2(x_i - x_p)(y_i - y_p) p_2 + \frac{(y_i - y_p)}{\rho} \Delta \theta_n \quad (5)$$

$$\Delta y_n = - \frac{(y_i - y_p)}{c} \Delta c + (y_i - y_p) r_1^2 k_1 + (y_i - y_p) r_1^4 k_2 + (y_i - y_p) r_1^6 k_3 + (r_1^2 + 2(y_i - y_p)^2) p_2 + 2(x_i - x_p)(y_i - y_p) p_1 - (y_i - y_p) s_{yn} \quad (6)$$

By combining the equations (1) and (2) and the self-calibration functional model equations (3-6), the extended observation equations result in the equations (7) for the DGR model and in the equations (8) for the LIM.

$$\begin{aligned} v_c &= Ax_{off} + B_s x_s + B_d x_d + Cx_g + Dx_{AP} - l_c ; P_c \\ v_s &= \quad \quad \quad x_s \quad \quad \quad - l_s ; P_s \\ v_d &= \quad \quad \quad \quad \quad x_d \quad \quad \quad - l_d ; P_d \\ v_g &= \quad \quad \quad \quad \quad \quad \quad x_g \quad \quad \quad - l_g ; P_g \\ v_{AP} &= \quad \quad \quad \quad \quad \quad \quad \quad \quad x_{AP} - l_{AP} ; P_{AP} \end{aligned} \quad (7)$$

where x_{AP} and P_{AP} denote the AP vector and their apriori weights vector.

$$\begin{aligned} v_c &= Ax_a + Bx_{INS} \quad \quad \quad + Cx_g + Dx_{AP} - l_c ; P_c \\ v_t &= \quad \quad \quad x_{INS} + B_s x_s + B_d x_d \quad \quad \quad - l_t ; P_t \\ v_s &= \quad \quad \quad \quad \quad \quad \quad x_s \quad \quad \quad - l_s ; P_s \\ v_d &= \quad \quad \quad \quad \quad \quad \quad \quad \quad x_d \quad \quad \quad - l_d ; P_d \\ v_g &= \quad x_g \quad \quad \quad - l_g ; P_g \\ v_{AP} &= \quad x_{AP} - l_{AP} ; P_{AP} \end{aligned} \quad (8)$$

2.3 AP Elimination Algorithm

The self-calibration algorithm presented here aims to determine the optimal set of APs for the optimal estimation of the object space coordinates of the measured image points. The adjustment procedure starts with the full parameter set and eliminates undeterminable parameters automatically in an iterative approach. The APs are introduced as free unknowns into the system. The major problem for parameter elimination is the

finding of robust criteria for rejection of undeterminable parameters. A stepwise parameter elimination algorithm proposed by Gruen (1985) is used here. The algorithm includes:

- Determinability check by analyzing the diagonal elements of the factorized normal matrix during Cholesky decomposition
- Analysis of the negative effect of each AP on the object space coordinates of the points by using the trace check algorithm of the covariance matrix
- Correlation analysis between the APs and the exterior orientation (EO) parameters, and also between the APs and the points' object space coordinates (an additional parameter having a correlation coefficient > 0.9 with the EO parameters or object space coordinates is considered as highly correlated and it is deleted from the system)
- Statistical significance tests under *Student's t distribution* ($t_\alpha = 0.05$) for the individual analysis of the APs; and under *Fisher distribution* ($F_\alpha = 0.05$) for the analysis of sub-sets of APs are applied. Four groups of APs, which consist of $(\Delta x_{pb}, \Delta x_{pf}), (\Delta y_{pb}, \Delta y_{pf}), (s_{yb}, s_{yn}, s_{yf}), (\Delta \theta_b, \Delta \theta_n, \Delta \theta_f)$, are tested with the F-distribution due to strong correlations between the parameters of the same group.

The camera constant (Δc), the affinity (s_{yn}) and the scan line inclination angle ($\Delta \theta_n$) parameters for the nadir CCD line, and the 3rd order lens distortion parameter (k_3) are deleted from the system permanently since they were highly correlated with EO parameters in the triangulation tests, which were performed with several STARIMAGER datasets and under several network conditions. The actual self-calibration algorithm runs with 12 APs. In case of k_3 this parameter is not sufficiently separable from k_1 and k_2 .

3. TEST DATA

3.1 Vaihingen/Enz Testfield ADS40 Dataset

The Vaihingen/Enz test site was established by the Institute for Photogrammetry (IFP), University of Stuttgart, in 1995 originally for the geometrical performance test of the DPA sensor. The test site itself is located about 20km north-west of Stuttgart in a hilly area providing several types of vegetation and land use, a mostly rural area with smaller forests and villages. There exist more than 200 signalized and natural control points in the area (Cramer, 2005).

An ADS40 test flight has been performed in summer 2004, as a joint project of Leica Geosystems and IFP Stuttgart with different flying heights. In addition to the standard ADS40 system installation, additional GPS/inertial units were installed during the flight. The performance analyses of these GPS/inertial systems and the triangulation results with the Orima software of Leica Geosystems and with the DGAP software of IFP Stuttgart are given by Cramer (2005). However, only the trajectory data acquired by the standard GPS/IMU installation of ADS40 including Applanix LN200 fiber-optic gyro based IMU (Litton) is used in this study. Some important camera parameters of the ADS40 are given in Table 1.

Table 1. ADS40 sensor and imaging parameters (Reulke et al., 2004)

Focal length	62.7 mm
Pixel size	6.5 μ m
Panchromatic line	2 x 12.000 pixels
Colour lines	12.000 pixels
Field of view (across track)	64°
Stereo angles	16°, 26°, 42°
Dynamic range	12 bit

The data acquired in the 1500m flight are used in our tests. The ADS40 test block parameters are given in Table 2. When the image scale is considered (1/24000), the average ground sample distance (GSD) of each pixel corresponds to 15.6 cm. The test dataset includes a total of 6 image strips, and 201 ground control points (Figure 2).

Table 2. ADS40 Vaihingen/Enz test block parameters

# of image strips (triplets)	6
Length/width of the TLS block	7.5 km x 4.8 km
GSD	15.6 cm
Date of acquisition	2004
# of GCPs	201
Apriori std. dev. of GCP coordinates	5 cm

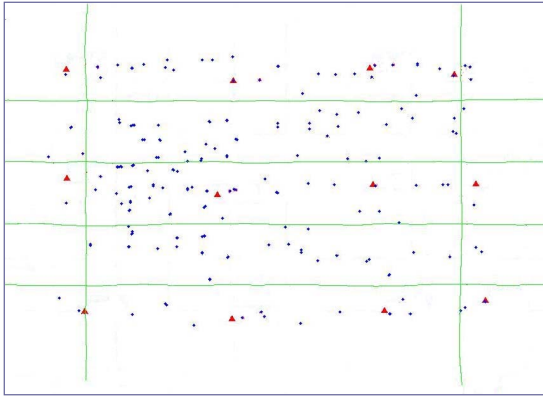


Figure 2: Image flight trajectories and ground control point distribution in the ADS40 Vaihingen/Enz dataset. The triangles represent the control point distribution for the 12 control points case. The remaining points are used as check points to compute the empirical accuracy.

In addition to image measurements in the PAN channels and the ground coordinates of the control points, the image trajectory files and the camera calibration data has been received from IFP, Stuttgart. The data has been tested under several numbers and distributions of control points using the LIM and the DGR models. In addition, the self-calibration algorithm has been applied.

First, the empirical accuracy of the given network has been computed using the differences of the given object space coordinates of the check points and the computed ones by performing spatial intersection, through the process of Direct Georeferencing. The RMSE values are under one pixel in X (12 cm) and Y (13 cm) directions, and slightly more than one pixel in height (18 cm). This indicates already the exceptional good accuracy of the measured orientation elements.

When the bundle adjustment with our DGR model is applied, there is a certain improvement in the RMSE values especially in Y and Z directions even without using control points (Figure 3). In this case, the trajectory elements are introduced as weighted unknowns. The apriori standard deviations for trajectory parameters are assumed to be equal to the above mentioned RMSE (X,Y,Z) values obtained from the space intersection process. With the use of the DGR model with 4 control points, the accuracy improves to 4.2 cm, 5.3 cm, and 6.4 cm in X, Y, and Z respectively. The same level of accuracy is obtained in case of 9 and 12 control points. When the self-calibration is applied, the DGR model accuracy results improve significantly in planimetry (Figure 3). The theoretical sigma values obtained from the covariance matrix and the estimated sigma-0 improve with self-calibration as well. The final AP set for the ADS40

self-calibration includes 11 parameters. The affinity parameter for the forward image (s_{yf}) is removed due to high correlations with the CCD line center displacement parameter in (x) for the forward image (Δx_{pl}).

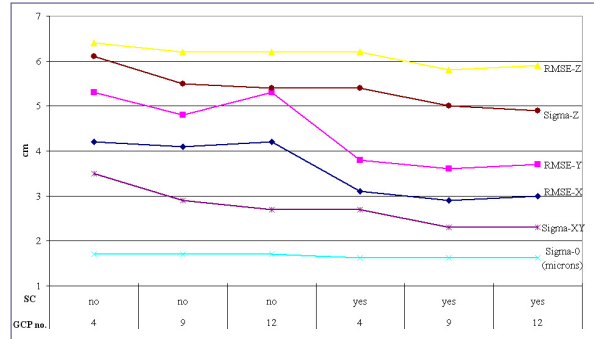


Figure 3. Vaihingen/Enz ADS40 dataset DGR model results.

The LIM results with different numbers of control points and two different number of orientation fixes are presented in Figures 4 and 5. With the LIM, when the number of control points increases, the height accuracy improves as well. However, for this dataset, the DGR results are in general slightly better than the LIM results. On the other hand, the positive effect of the self-calibration parameters is observed in the planimetric accuracy results. The negative effect on the height accuracy is not understood yet and should be further analyzed. The sigma-0 parameter improves to 1.17 μm with use of self-calibration with LIM having 8 orientation fixes (Figure 5).

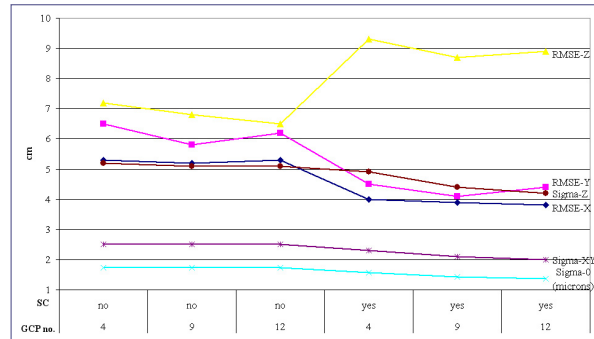


Figure 4. Vaihingen/Enz ADS40 dataset LIM results with 4 orientation fixes.

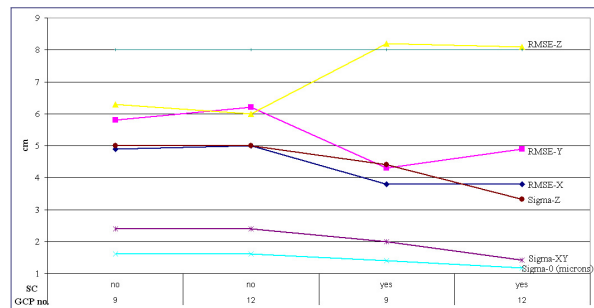


Figure 5. Vaihingen/Enz ADS40 dataset LIM results with 8 orientation fixes.

3.2 Yoriichio Testfield STARIMAGER SI-100 Dataset

The STARIMAGER system of former Starlabo Corp. is composed of eight major subsystems (imaging, data pre- and

post-processing, trajectory data recording, data storage systems, etc.), which are discussed in Chen et al. (2003). The imaging system typically has three major subassemblies: stabilizer, INS, and the TLS. The TLS system produces seamless high-resolution images (5 - 10 cm footprint on the ground) in three viewing directions (forward, nadir and backward). As the first engineering model of the STARIMAGER, the SI-100 camera configuration contains three times three parallel one-dimensional CCD focal plane arrays, with 10 200 pixels of 7 μ m each (Gruen and Zhang, 2002). The sensor parameters of the SI-100 camera are given in Table 3.

Table 3. SI-100 sensor and imaging parameters

focal length	60.0 mm
number of pixels per array	10 200
pixel size	7 μ m
number of CCD focal plane arrays	3
stereo view angle	21/42° *
field of view	61.5°
instantaneous field of view	0.0065°
scan line frequency	500 HZ

* forward-nadir/forward-backward stereo view angle

Three parallel SI-100 image strips acquired over the Yoriichio testfield are used for the self-calibration tests. The data configuration is given in Table 4. The image strips and control point distribution are shown in Figure 6.

Table 4. SI-100 Yoriichio test block parameters

# of image strips (triplets)	3
Length/width of the TLS block	10km x 1.4km
GSD	7 cm
Date of acquisition	02/02/2002
# of GCPs	61
Apriori std. dev. of GCP coordinates	3 cm
Total # of tie points	182

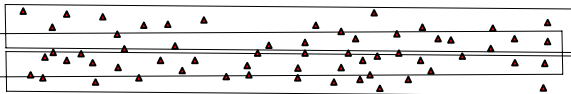


Figure 6. Three SI-100 image triplets in the Yoriichio area that are used for multiple strips block adjustment tests. The lines denote the strip edges and the triangles denote the measured GCPs.

The Yoriichio testfield SI-100 data triangulation results with the DGR model are given in Figure 7. From 6 to 15 GCPs, the RMSE values improve slightly in planimetry and in height. When self-calibration is applied, the major improvement appears in the standard deviations and in sigma naught values. The RMSE values however do not show an improvement. The full set of APs with 12 parameters are included in the adjustment.

The triangulation accuracy results with the LIM are presented in Figures 8 and 9. The tests vary with the number of GCPs, and the orientation fixes, and with the application of self-calibration. In comparison to the DGR model, a higher number of control points is necessary to use the LIM. However, contrary to the DGR results, using more control points improves the accuracy significantly. When self-calibration is applied, the RMSE values and the standard deviations improve in all LIM tests. The final AP set includes all 12 parameters. The best accuracy results in the Yoriichio testfield data are obtained with the LIM with 30

orientation fixes, and using 30 GCPs. The sigma naught results in one pixel for this test configuration.

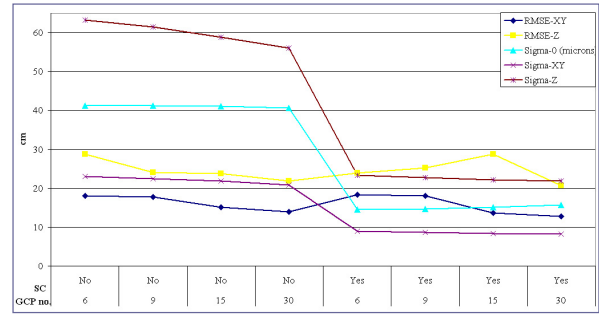


Figure 7. Yoriichio SI-100 dataset DGR model results.

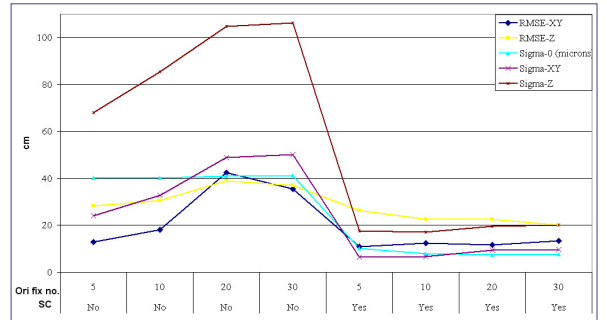


Figure 8. Yoriichio SI-100 dataset LIM results with 15 GCPs.

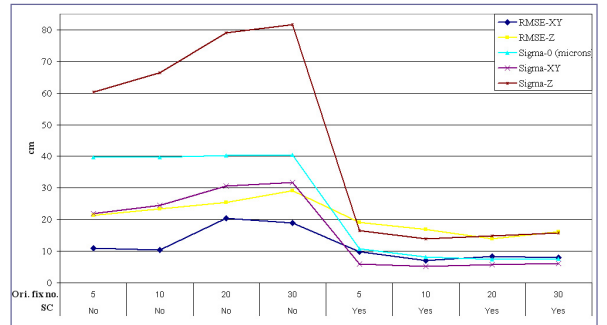


Figure 9. Yoriichio SI-100 dataset LIM results with 30 GCPs.

4. CONCLUSIONS

Potential systematic error sources of linear array CCD cameras are identified and tested. In our triangulation tests the camera constant (Δc), affinity (s_{yn}) and scan line inclination angle ($\Delta \theta_n$) parameters for the nadir CCD line, and the 3rd order lens distortion parameter (k_3) are found to be too instable to improve the system accuracy. The final self-calibration model includes 12 additional parameters. The parameter elimination strategy proposed by Gruen (1985) works efficiently.

Accuracy and precision aspects of our two trajectory models, the DGR and the LIM, are evaluated with the ADS40 data and the STARIMAGER data acquired over two different testfields. In the ADS40 testfield data case, very accurate trajectory data are provided by the GPS/IMU system. The triangulation accuracy results with the DGR and the LIM models are about at the same level. However, the use of self-calibration improves the accuracy in terms of RMSE values in planimetry, the standard deviations of the estimated object space coordinates, and the sigma naught. Only one parameter needed to be deleted from the

system due to high correlations. According to the trace check algorithm, the remaining additional parameters do not disturb the system's reliability.

In the SI-100 test data case, the DGR model requires less control points, but the accuracy remains the same with more control points. The self-calibration with the DGR model improves the sigma naught and the standard deviations only. The LIM models the trajectory errors better, although more control points are needed. In addition, the additional parameters help to improve the overall system accuracy in all LIM tests. A high number of orientation fixes provide only slightly better triangulation accuracy. However more control points are needed to keep the system stability in this case.

Both datasets used here are of somewhat uncharacteristic type in the sense that the Vaihingen data has a very high a priori accuracy of the orientation elements, while the Yoriichio block has to cope with insufficient image quality, bad definition of signalized points and problems in GPS/INS processing.

Therefore, the results shown here should be examined with some care and cannot necessarily be generalized.

REFERENCES

- Beyer, H.A., 1992. Geometric and Radiometric Analysis of a CCD-Camera Based Photogrammetric Close-Range System. Dissertation, No. 9701, ETH, Zurich.
- Boerner, A., Reulke, R., Scheele, M., Terzibaschian, Th., 1997. Stereo Processing of Image Data from an Airborne Three-Line CCD Scanner. The 3rd International Airborne Remote Sensing Conference and Exhibition, 7-10 July, Copenhagen, Denmark.
- Brown, D.C., 1971. Close-Range Camera Calibration. *Photogrammetric Engineering*, 37 (8), pp. 855-866.
- Brown, D.C., 1976. The Bundle Adjustment – Process and Prospects. Invited Paper to the XIIIth Congress of the ISPRS Comm. III, Helsinki.
- Chen, T., Shibasaki, R., Morita, K., 2001. High Precision Georeference for Airborne Three-Line Scanner (TLS) Imagery. 3rd International Image Sensing Seminar on New Developments in Digital Photogrammetry, Sept. 24-27, Gifu, Japan, pp. 71-82.
- Chen, T., Shibasaki, R., Murai, S., 2003. Development and Calibration of the Airborne Three-Line Scanner (TLS) Imaging System. *ASPRS Journal of PE&RS*, vol. 69, no. 1, pp. 71-78.
- Cramer, M., 2005. 10 Years ifp Test Site Vaihingen/Enz: An Independent Performance Study. *Photogrammetric Week '05*, Wichmann, Heidelberg, pp. 79-92.
- Ebner, H., 1976. Self-calibrating Block Adjustment. Invited Paper to the XIIIth Congress of the ISPRS Comm. III, Helsinki.
- Ebner, H., Kornus, W., Ohlhof, T., 1992. A Simulation Study on Point Determination for The MOMS-02/D2 Space Project Using an Extended Functional Model. *IAPRS*, Washington, D. C., Vol. 29, Part B4, pp. 458-464.
- Fraser, S. C., 1997. Digital Camera Self-calibration. *ISPRS Journal of Photogrammetry and Remote Sensing*, vol. 52, pp. 149-159.
- Gruen, A., 1978. Progress in Photogrammetric Point Determination by Compensation of Systematic Errors and Detection of Gross Errors. *Nachrichten aus dem Karten- und Vermessungswesen*, Series II, 36, 113-140.
- Gruen, A., 1985. Data Processing Methods for Amateur Photographs. *Photogrammetric Record*, 11 (65), pp. 567-579.
- Gruen, A., Beyer, H.A., 2001. System Calibration Through Self-Calibration. *Calibration and Sensor Orientation of Cameras in Computer Vision*, Eds. Gruen, Huang, Springer-Verlag Berlin, Heidelberg, pp.163-193.
- Gruen, A., Zhang, L., 2002. Sensor modelling for aerial mobile mapping with Three-line Scanner (TLS) imagery. Symposium of Commission II, Integrated System for Spatial Data Production, Custodian and Decision Support, 20-23 Aug., Xian, China.
- Gruen, A., Zhang, L., 2003. Sensor Modeling for Aerial Triangulation with Three-Line-Scanner (TLS) Imagery. *Journal of Photogrammetrie, Fernerkundung, Geoinformation*, 2/2003, pp. 85-98.
- Haala, N., Stallmann, D., Cramer, M., 1998. Calibration of Directly Measured Position and Attitude by Aerotriangulation of Three-Line Airborne Imagery. *The International Archives of Photogrammetry and Remote Sensing*, Budapest, Vol. 32, Part 3, pp. 23-30.
- Murai, S., Matsumoto, Y., 2000. The Development of Airborne Three Line Scanner with High Accuracy INS and GPS for Analysing Car Velocity Distribution. *The International Archives of Photogrammetry and Remote Sensing*, Amsterdam, Vol. 33, Part B2, pp. 416-421.
- Reulke, R., Franke, K-H., Fricker, P., Pomierski, T., Sandau, R., Schoenermark, M., Tornow, C., Wiest, L., 2000. Target Related Multispectral and True Color Optimization of the Color Channels of the LH Systems ADS40. *The International Archives of Photogrammetry and Remote Sensing*, Amsterdam, Vol. 33, Part B1, pp. 244-250.
- Reulke, R., Tempelmann, U., Stallmann, D., Cramer, M., Haala, E., 2004. Improvement of Spatial Resolution with Staggered Arrays as used in the Airborne Optical Sensor Leica ADS40. *ISPRS Congress 2004*, Volume 35, Part B, Istanbul, Turkey, digital on CD, 4 pages.
- Sandau, R., Braunecker, B., Driescher, H., Eckardt, A., Hilbert, S., Hutton, J., Kirchhofer, W., Lithopoulos, E., Reulke, R., Wicki, S., 2000. Design Principle of The LH Systems ADS40 Airborne Digital Sensor. *The International Archives of Photogrammetry and Remote Sensing*, Amsterdam, Vol. 33, Part B1, pp. 258-265.
- Wewel, F., Scholten, F., Gwinner, K., 1999. High Resolution Stereo Camera (HRSC) – Multispectral Data Acquisition and Photogrammetric Data Processing. 4th International Airborne Remote Sensing Conference and Exhibition, Ottawa, Canada, Vol. I, pp. 263-272.

ACKNOWLEDGEMENT

The authors would like to thank Starlabo Corporation, Tokyo for their project support and the provision of the Yoriichio testfield datasets. Thanks also go to Leica Geosystems and the IFP Stuttgart for providing the Vaihingen/Enz dataset and their support.